Phase ratio estimations from true color images.

Eric PIRARD[1] and Simone TARQUINI[2].

[1] Université de Liège. MICA_ULg. Avenue des Tilleuls. 45 4000 LIEGE (BELGIUM)
[2] Univ. degli Studi di Pisa. Dip. Sc. della Terra. Via S. Maria. 53 56100 PISA (ITALY)

Introduction

Quantitative chemical analyses are particularly well suited for characterising processes involving individual mobility of the chemical elements. On the other hand, the basic building blocks of most mineral and material processing operations are solids and a true quantitative analysis in terms of mineral phase ratios (modal analysis) is clearly more helpful in understanding such processes. Among the available techniques for estimating mineral phase ratios, image analysis is probably the most promising because it theoretically allows to adress elated problems like : granulometry, intergrowth, preferential orientations....

Any quantitative phase ratio estimation procedure implies the following steps :

a) Positionning of probes (planes, lines, etc.) at random in the 3-D volume to be estimated.
b) Classification of these probes with respect to the mineral phases they belong to.

Stereology

Since Delesse (1848) it is known that the following property holds :

$$A_A = V_V$$

Basically, this means that the volumic fraction (V_V) of a mineral is unbiasedly estimated by the mean area fraction (A_A) of this mineral from a series of random planes. For practical purposes, volumic fractions are commonly estimated from area fractions measured in sections. Provided we are given enough random sections from a given material, no further stereological correction will be necessary for estimating true phase ratios in 3-D.

Segmentation

Area fractions in sections are estimated with an image analyser in exactly the same way as they are with the point-counting technique. The point-counting technique relies on a skilled operator being able to identify mineral species from their optical characteristics for each given point on the grid. In the same manner, image analysis requires that the computer be able to automatically classify pixels within an image as corresponding to a given mineral. Automatic recognition of mineral signatures is still very limited. Although the most promising technique in this respect is probably related to X-Ray fluorescence (EDX), it is worthwhile trying to develop as much as possible from optical signals. The widespread availability of optical equipments and the very affordable cost of video compatible equipments stimulates this effort.

The best sensor used for acquiring true color information in standard video format is a 3-CCD color camera with direct RGB output (Connolly and Leung, 1995). With a standard frame grabber, the result of digitizing an RGB signal is a set of three images (Red / Green / Blue) with 512 x 512 pixels resolution and a pixel depth of 8 bits (values between 0 and 255 representing grey levels in each channel) (Figure1).

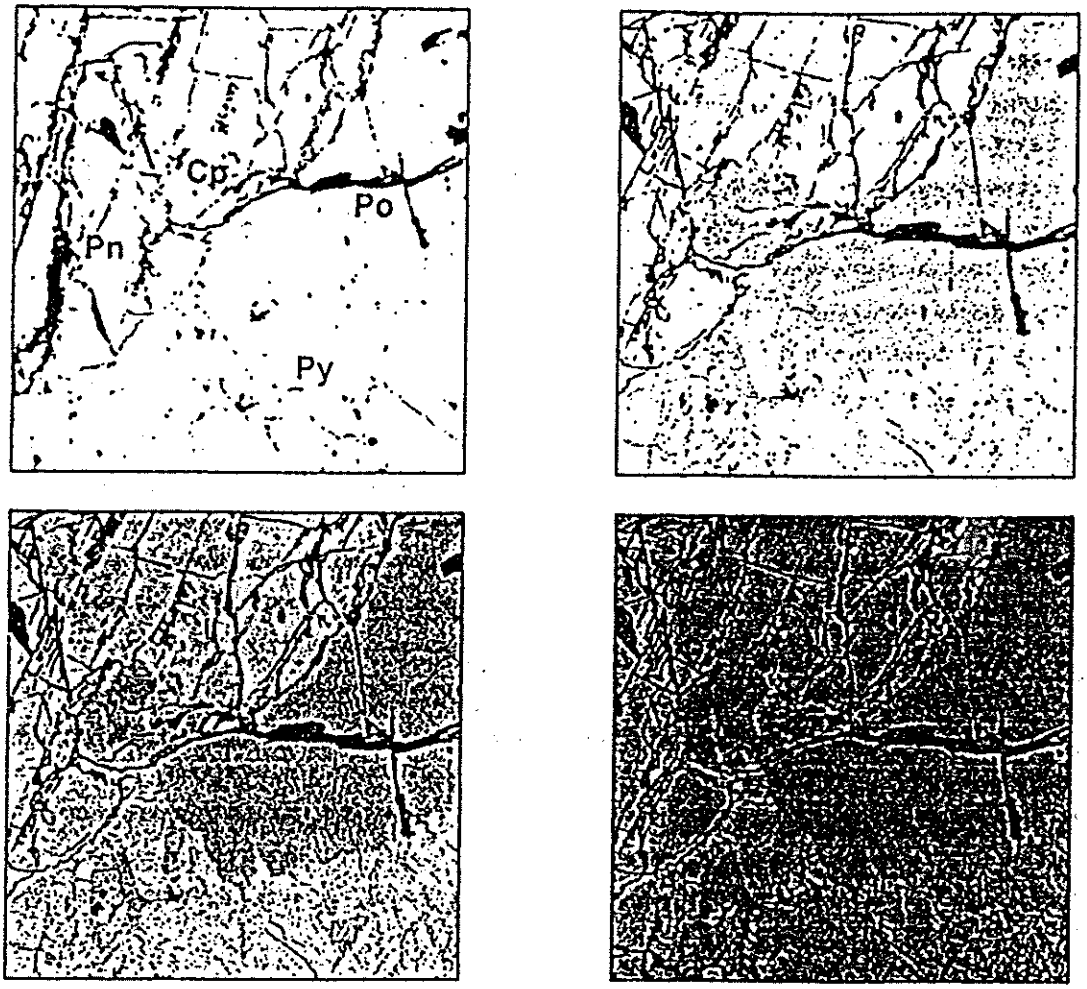

Figure 1. Image of a sulphide mineralisation from Sudbury displaying Pyrrhotite (Po), Chalcopyrite (Cp), Pyrite (Py) and Pentlandite (Pn). From left to right: B&W image (2/3" camera); Red, Green and Blue images (1/2" 3-CCD camera).

Reflectance spectra vs RGB video

Reflectance spectra have been compiled for a wide range of ore minerals (Picot and Johan, 1977 ; Criddle and Stanley, 1993). Such spectra are acquired in normalized conditions that are not comparable to the signal output from a video camera using a halogen bulb as light source. Table 1 compares compiled reflectance values with the means and standard deviations of RGB intensities computed from a window of 20x20 pixels positionned on each mineral. One must keep in mind that the RGB channels of a video camera do not correspond to the same wavelengths and have broad spectral bandwidth.

	700 nm	600 nm	540 nm	420 nm	Red		Green		Blue	
					$\overline{N_R}$	σ_R	$\overline{N_G}$	σ_G	$\overline{N_B}$	σ_B
Chalcopyrite	42	39	35	17	168	4.5	138	5.4	76	4.7
Pentlandite	56	52	49	35	187	3.1	156	3.3	105	2.9
Pyrite	57	55	54	40	192	3.2	173	3.7	116	3.2
Pyrrhotite	41	39	35	29	165	2.6	138	3.0	94	2.3

Table 1 Reflectance values under monochromatic light (Picot & Johan,1977) and grey level statistics (mean, standard deviation) for each channel.

From results in table 1 it appears that Pyrrhotite and Chalcopyrite are much more differentiated in the blue channel than in any other one. In practice, thresholding the blue image (Figure 2) will allow a correct phase segmentation that would otherwise be unpracticable from

the B&W image (Figure 3). Distinguishing between Pyrite and Pentlandite appears to be a more complex situation.

Figure 3. Result from thresholding the Blue channel. Pyrrhotite is clearly distinguished from Chalcopyrite.

Figure 2. Result from thresholding the B&W image. Pyrrhotite and Chalcopyrite are not separable.

Assuming a reasonable normality for the reflectance peaks, one might threshold each channel using a 95% confidence interval $\left[\overline{X} - 2.\sigma, \overline{X} + 2.\sigma\right]$. Logical AND is performed on the three binary images of the same phase resulting from the segmentation. This operation amounts to label as pentlandite all pixels falling within a parallelepiped in the RGB hyperspace (Figure 4). If we repeat this operation for each of the n minerals identified in the image we obtain a set of n binary images (Figure 5).

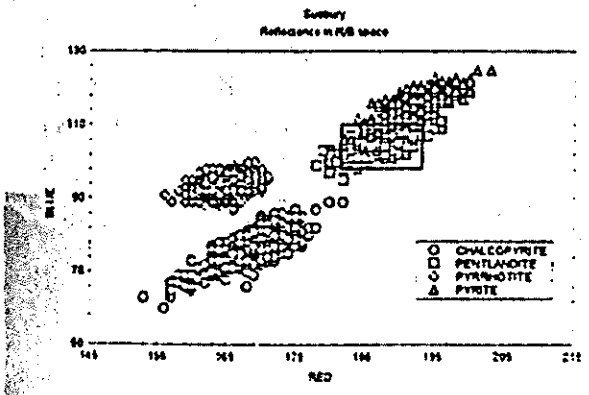

Figure 4. Scatterplot of 4*400 pixels in the Red Blue space. Pixels within the thresholds (rectangle) are labelled as pentlandite.

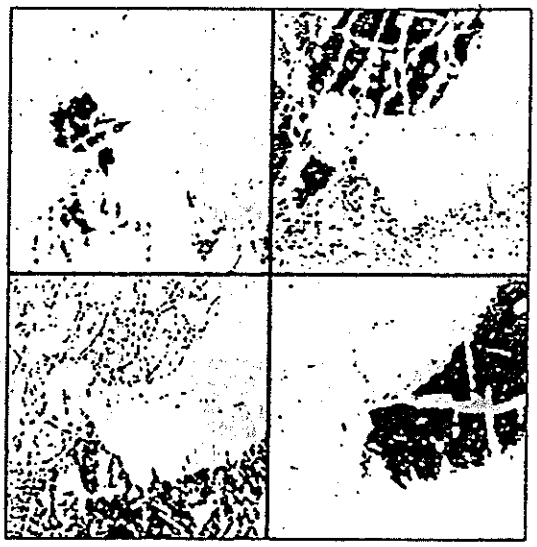

Figure 5. Binary images of pixels classified as Chalcopyrite, Pentlandite, Pyrite and Pyrrhotite.

Spectral undetermination

Spectral undetermination results either from pixels never having been selected (0) or from pixels having been selected more than once in the thresholding process (e.g. both in the pyrite and pentlandite images).

Undetermination is a logical result of polishing artefacts and optical aberrations . Most scratches, pits, fractures and microhardness fringes appear as unselected pixels (0) whereas uneven lightning, bireflectance, compositional variations and spectral overlapping often induces multiple selection (A+B) (Figure 6).

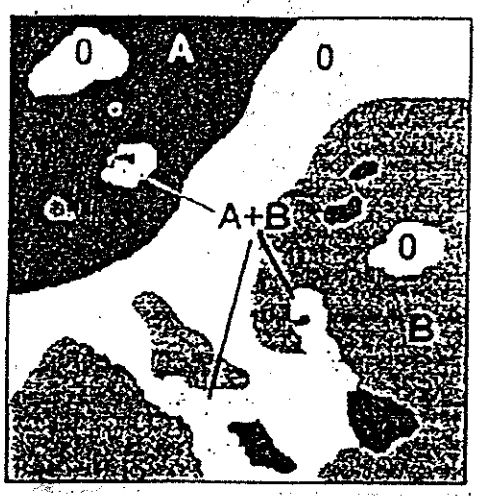

Figure 6. Exemple of composite image with spectral attribution of pixels.

Multivariate classification techniques (Goldberg & Shlien, 1978) may appear more powerful than a simple threefold univariate threshold, but the aim of the present approach is to obtain only a dense subset of perfectly classified pixels and solve undetermination by considering an additional spatial criterion.

Spatial undetermination

A closer look at the composite image reveals a complex spatial relationship between classified and unclassified pixels (Figure 6). Zero-valued pixels appear either as being holes (pits) within a mineral grain or as fractures crossing the image. Ambiguous pixels (A + B) appear either within a pure phase A (or phase B) zone or at the contact between B and A grains. Finally, well classified pixels form massive clusters in the heart of pure grains but may also appear as speckles within another phases (Figure 8).

Instead of considering these speckles as being inclusions or exsolutions it is often more realistic to consider them as spectral noise and add these pixels to the unclassified pixels list. In practice, this is realised by performing a dilation of size « d » on each one of the n binary images. As a consequence, all pixels lying within a distance of less than d pixels to a phase A / phase B transition are now labelled as A+B and added to the undetermined pixels(Figure 7a-b).

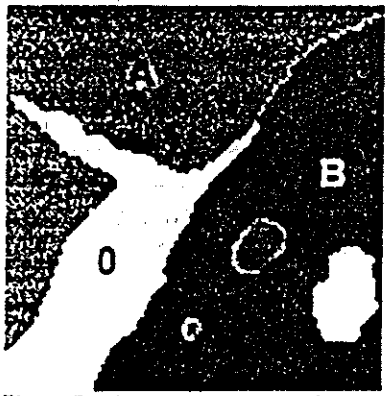

Figure 7a. Composite image with spectrally undetermined regions.

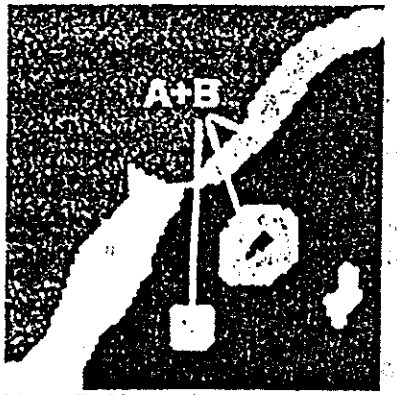

Figure 7b. New undeterminations resulting from dilation of A and B.

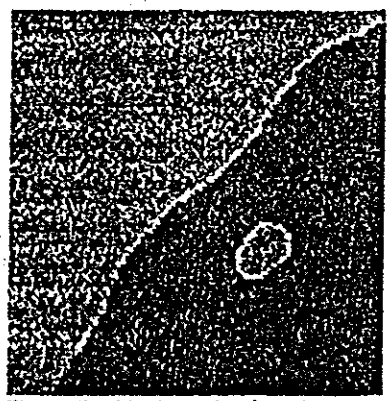

Figure 7c. Final result of geodesic propagation over undetermined regions.

Geodesic propagation

Considering that the final result has to be an image where no pixels are left unclassified, a geodesic propagation (Coster & Chermant, 1985) is performed to classify ambiguous domains. The practical result of this is that all unclassified pixels are assigned a value corresponding to the code of the nearest classified pixel (Figure 7c). Thanks to the previous dilation process, the geodesic propagation step fills in undetermined A−B zones and acts as a filter removing noisy pixels within well classified domains. This kind of filtering is considered as a contextual filter, because it selectively removes isolated pixels lying within well classified regions without affecting isolated pixels scattered in an undetermined region of the image (Figure 8).

Conclusion

True color information, captured via a 3-CCD camera contributes to improve mineral segmentation in image analysis. Rather than using multivariate segmentation procedures, the proposed method relies on simple univariate thresholds giving a composite image with a reasonable amount of unclassified pixels. A further geodesic propagation reassigns pixels to mineral phases on a spatial rather than spectral basis. Minerals showing a difference of 5% reflectance in one of the three bands (R/G or B) are correctly segmented and allow for a p ·ise phase ratio estimation (Figure 9).

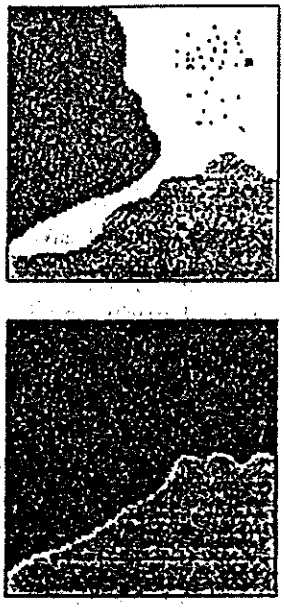

Figure 8. The upper image shows speckles of the black phase either within the grey phase or within the undetermined region. The lower image illustrates how the contextual filter uses only the latter ones as germs of the propagation process and removes those within the grey phase.

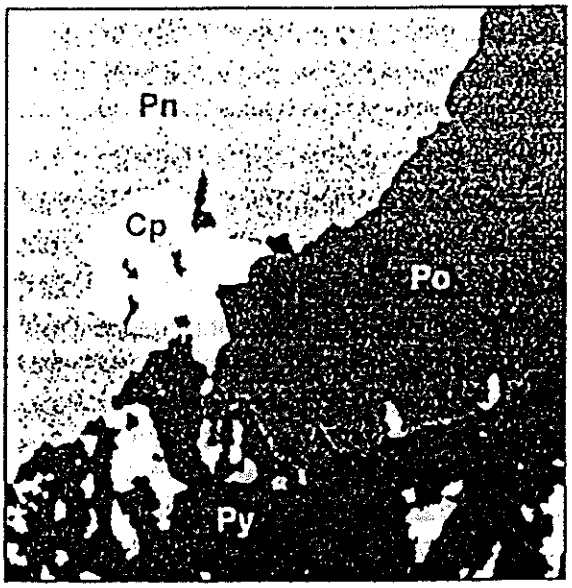

Figure 9. Final result of segmentation of the RGB channels in figure 1.

Bibliographie

Connolly C. and Leung T.W. 1995. Industrial colour inspection by video camera. *Image Processing and its Applications*. IEE Conf. Publ. n°410. pp 672-676:

Coster M. & Chermant J. L. 1985. *Precis d'Analyse d'Image*. éditions du CNRS. Paris:

Criddle A. J. & Stanley C. J. 1993 *Quantitative data file for Ore Mineral: third edition* Chapman & Hall. London:

Goldberg M. & Shlien S. 1978. *A Clustering Scheme for Multispectral Images*. IEEE Transactions-SMC. Vol. SMC-8. N°2. p. 86-92:

Picot P. & Johan Z. 1977. *Atlas des Mineraux Metalliques*. Editions du B.R.G.M. Paris: